World Academy of Science, Engineering and Technology
International Journal of Energy and Power Engineering
Vol:4, No:5, 2010

Fractal Patterns for Power Quality Detection Using Color Relational Analysis Based Classifier

[1]Chia-Hung Lin, [1]Mei-Sung Kang, [2]Cong-Hui Huang, and [3]Chao-Lin Kuo

***Abstract*—**This paper proposes fractal patterns for power quality (PQ) detection using color relational analysis (CRA) based classifier. Iterated function system (IFS) uses the non-linear interpolation in the map and uses similarity maps to construct various fractal patterns of power quality disturbances, including harmonics, voltage sag, voltage swell, voltage sag involving harmonics, voltage swell involving harmonics, and voltage interruption. The non-linear interpolation functions (NIFs) with fractal dimension (FD) make fractal patterns more distinguishing between normal and abnormal voltage signals. The classifier based on CRA discriminates the disturbance events in a power system. Compared with the wavelet neural networks, the test results will show accurate discrimination, good robustness, and faster processing time for detecting disturbing events.

***Keywords*—**Power Quality (PQ), Color Relational Analysis (CRA), Iterated Function System (IFS), Non-linear Interpolation Function (NIF), Fractal Dimension (FD).

Open Science Index, Energy and Power Engineering Vol:4, No:5, 2010 waset.org/Publication/12617

I. Introduction

POWER quality (PQ) disturbances could cause distorted waves and degrade the voltage quality to impair the operation of electrical apparatus. These disturbances cause problems, such as overheating, motor failures, inaccurate metering, and mis-operation of protective equipment, which can be affected by harmonics, voltage sag, voltage swell, and momentary interruptions. Voltage disturbances and harmonic sources could affect the branch currents and node voltages, and could downgrade the service quality. PQ detection is essential for the reliable distribution of electric energy. To ensure the PQ, power disturbances detection becomes important as well to further detect the location and disturbance types. This study provides a classifier for detection with limited partially observable measurement for part of the networks.

In literatures [1]-[10], many techniques have been able to monitor, locate, and identify disturbances by measurement instruments and automatic detection approaches. Measurement instruments could collect large amounts of measured data such as voltage waveforms, current waveforms, complete harmonic spectrum, total harmonic distortion, and occurrence times. These data are applied for signal processing and analysis. With the frequency-domain techniques [3]-[10],Fast Fourier Transformation (FFT), Short-time Fourier Transformer (STFT),and wavelet transformation (WT) for power quality analysis has been presented.

[1]Chia-Hung Lin and Mei-Sung Kang are with the Department of Electrical Engineering, Kao-Yuan University, Lu-Chu Hsiang, Kaohsiung county 821, Taiwan, e-mail: kmswmy@cc.kyu.edu.tw

[2]Cong-Hui Huang is with the Department of Automation and Control Engineering, Far-East University, Hsin-Shih Township, Tainan County, 744, Taiwan.

[3]Chao-Lin Kuo is with the Department of Electrical Engineering, Far-East University, Hsin-Shih Township, Tainan County, 744, Taiwan.

However, the choices for size of the time window affect both the frequency and time resolution when using FFT and STFT. WT functions cascaded low-pass or high-pass filters and down/up-sampling operations to generalize several frequency bands. This analysis is robust to time-varying signal analysis and it can point out occurrence time. A signal is described in a time-scale domain, and analogous to a time-frequency domain. Significant features are suited to classify different patterns at specific dilation and translation coefficients, which are obtained at specific coefficients with a trial procedure of wavelet decomposition. Then artificial neural networks (ANN) are designed to classify different types of disturbances, such as multilayer neural networks and wavelet neural networks (WNNs) [5]-[10].

The above literatures concerning the frequency- domain features contain valuable information for PQ detection, and ANN proposes a classifier for signal analysis and pattern recognition. The ANN method can allow non-linear classification, but the local minimum problem, slow learning speed, architecture determination, and the weight interferences between different patterns are the major limitations. To overcome the drawbacks, fractal analysis is an approach with fractal dimensions (FDs) and results the data self-similarity [11]. Fractal patterns are used to construct the information from time-series signals. Iterated function system (IFS) is proposed for modeling the non-linear interpolation functions (NIFs) [12]-[15], which require fewer map parameters for constructing fractal patterns of normal and abnormal signals [16]. For pattern recognition, color relational analysis (CRA) is applied to develop a classifier for PQ detection. It has a flexible pattern mechanism with add-in and delete-off features without parameter adjustment, and does not demand strict statistical methods and inference rules. For a sample power system, computer simulations will show computational efficiency, accurate discrimination, and good robustness for different tests.

II. Mathematical Method

A. Fractal Dimension Transformation (*FDT*)

The fractal method of modeling data is based on selecting interpolation points from the sampling data and creating IFS maps to interpolate between these points. An IFS has been proposed for image compression and signal modeling, and can produce family functions with different fractal dimensions (FDs). It is a finite set for contraction patterns, and has been used to create images, various waveforms and geometric patterns for image classification and signal analysis [11]-[12]. IFS is implemented with similarity maps, and the resulting data are self-similar. Apply a function or data sequence $x[t]$, t=1, 2, 3, …, N, the pth interpolation map W_p, p=1, 2, 3, …, P, IFS model can be presented as

$$W_p\left(\begin{bmatrix} t \\ x[t] \end{bmatrix}\right)=\begin{bmatrix} a_p & b_p \\ c_p & d_p \end{bmatrix}\begin{bmatrix} t \\ x[t] \end{bmatrix}+\begin{bmatrix} e_p \\ f_p \end{bmatrix} \quad (1)$$

$$\begin{cases} W_p(t)=a_p t+b_p x[t]+e_p \\ W_p(x[t])=c_p t+d_p x[t]+f_p \end{cases} \quad (2)$$

where $W_p(\bullet)$ maps the data sequence $x_p[t]$ onto the subsequences with N_p sampling data in the interval $[N_{p1},N_{p2}]$, the so-called non-linear interpolation function (NIF). The integrated map can be constructed side by side. The fractal method includes two stages: first to determine the interpolation points and FDs, and second to determine the best remaining map parameters, such as a_p, b_p, c_p, d_p, e_p, and f_p. These parameters can be solved by minimizing the sum of squared errors between the transformed data and the original data in the pth map, and can be justified by the Collage Theorem [13]-[15]:

$$e_p=\sum_{t=1}^{N_p}(W_p(x_p[t])-x_p[t])^2 \quad (3)$$

where $n=\text{int}[(\frac{t-N_{p1}}{N_{p2}-N_{p1}})(N-1)]$, $N_p=N_{p2}-N_{p1}+1$, and $N=N_1+N_2+N_3+\cdots+N_p+\cdots+N_P$. To improve the constraint, non-linear terms as sinusoidal functions can be added to $W_p(\bullet)$, which makes the signal modeling more flexible for processing non-linear or irregular signals. The NIF can be represented as

$$W_p(x_p[t])=c_p n+d_p x_p[t]+f_p+g_p\sin(\frac{\pi n}{N}) \quad (4)$$

The model projects the mapped data onto a sinusoidal interpolation. In this study, a fractal pattern of voltage or current signal can be adjoined with positive-half and negative-half cycles. The NIF with FDs will change the signals into fractal patterns at different scale parameters. Voltage and current are one-dimension time-varying signals in the time-domain. FD must be a parameter between 1 and 2 for processing one-dimensional signals. The NIF can be modified as [16]

$$\varphi_{pt}(x_p[t])=c_p n'+d_p\Delta x_p[t]+f_p+g_p\sin(\frac{\pi n'}{D}) \quad (5)$$

$$n'=(\frac{D-1}{N_p-1})t \quad (6)$$

where D is the FD, $\Delta x_p[t]=x_p[t]-x_p^{nor}[t]$, $x_p^{nor}[t]$ is the sequence of samples obtained from fundamental wave in the time-domain. Equation (5) is called the fractal dimension transformation (FDT). The Katz's algorithm is used to estimate the FD [12], as

$$D=\frac{\log_{10}(N)}{\log_{10}(N_d)}, \text{ and } 0<N_d<N \quad (7)$$

$$N_d=\max\{N_1,N_2,\cdots,N_p,\cdots,N_P\} \quad (8)$$

where N_p is the number of sampling points in the pth segment; N is the total number of sampling points ($N=N_1+N_2+N_3+\cdots+N_p$); N_d is the maximum number of sampling points among the P segments. The remaining map parameters c_p, d_p, f_p, and g_p can be solved by

$$\sum_{t=1}^{N_p}[S_t\cdot S_t^T]\begin{bmatrix} c_p \\ d_p \\ f_p \\ g_p \end{bmatrix}=\sum_{t=1}^{N_p}S_t\cdot x_p[t] \quad (9)$$

$$S_t=\begin{bmatrix} n' & \Delta x_p[t] & 1 & \sin(\frac{\pi n'}{D}) \end{bmatrix}^T \quad (10)$$

Apply sequence data $\Delta x_p[t]$ are the sampling data from the voltage and current signals. The fractal patterns can be reconstructed as

$$\Phi(\varphi_{pt})=\bigcup_{p=1}^{P}abs[\varphi_{pt}(x_p[t])],\ t=1, 2, 3, \ldots, N_P \quad (11)$$

The pattern Φ can be also represented as $\Phi=[\varphi_{11},\varphi_{12},\varphi_{13},\ \ldots\ ,\varphi_{1N1}|\varphi_{21},\varphi_{22},\varphi_{23},\ \ldots,\varphi_{2N2}|\ldots|\varphi_{P1},\varphi_{P2},\varphi_{P3},\ \ldots,\varphi_{PNP}]=[\phi_1,\phi_2,\phi_3,\ \ldots,\phi_i,\ \ldots,\phi_N]$, $i=1, 2, 3, \ldots, N$. Equations (5) and (6) are used to extract the features, and (11) is utilized to construct the fractal patterns of disturbances, including harmonics (*h*), voltage sags (*sa*), voltage swells (*sw*), sags or swells involving harmonics (*hsa*/*hsw*), and voltage interruptions (*int*).

B. Color Relational Analysis (*CRA*)

Pattern recognition is a research that aims to classify data/patterns based on behavioral characteristics, or on statistical information extracted from the patterns. These patterns to be classified are usually groups of measurements or observations, defining finite points in an appropriate multi-dimensional space. Artificial intelligence methods have concerned with the classification or description of observations. Based on similarity and dissimilarity, relational measurement is a method for determining the relationship between reference pattern and other comparative patterns. Color relation analysis (CRA) is conducted to classify patterns. Assume a reference pattern $\Phi_r=[\phi_1(0),\ \phi_2(0),\ \phi_3(0),\ \ldots,\ \phi_i(0),\ \ldots,\ \phi_N(0)]$,and K comparative patterns $\Phi_c(k)=[\phi_1(k),\ \phi_2(k),\ \phi_3(k),\ \ldots,\ \phi_i(k),\ \ldots,\ \phi_N(k)]$, $k=1, 2, 3, \ldots, K$, can be represented as [17]

$$\Phi_r(0)=[\phi_1(0)\ \ \phi_2(0)\ \ \cdots\ \ \phi_i(0)\ \ \cdots\ \ \phi_N(0)] \quad (12)$$

$$\begin{bmatrix} \Phi_c(1) \\ \Phi_c(2) \\ \vdots \\ \Phi_c(k) \\ \vdots \\ \Phi_c(K) \end{bmatrix}=\begin{bmatrix} \phi_1(1) & \phi_2(1) & \cdots & \phi_i(1) & \cdots & \phi_N(1) \\ \phi_1(2) & \phi_2(2) & \cdots & \phi_i(2) & \cdots & \phi_N(2) \\ \vdots & \vdots & \ddots & \vdots & \ddots & \vdots \\ \phi_1(k) & \phi_2(k) & \cdots & \phi_i(k) & \cdots & \phi_N(k) \\ \vdots & \vdots & \ddots & \vdots & \ddots & \vdots \\ \phi_1(K) & \phi_2(K) & \cdots & \phi_i(K) & \cdots & \phi_N(K) \end{bmatrix} \quad (13)$$

Open Science Index, Energy and Power Engineering Vol:4, No:5, 2010 waset.org/Publication/12617

where N is the dimensional space in one pattern; K is the number of comparative pattern. Compute the absolute deviation of reference pattern Φ_r and k comparative pattern $\Phi_c(k)$ by

$$\Delta\phi_i(k) = |\phi_i(0) - \phi_i(k)| \tag{14}$$

Compute the index $ED(k)$, as

$$ED(k) = \sqrt{\sum_{i=1}^{N} (\Delta\phi_i(k))^2} \tag{15}$$

where $ED(k)$ is the Euclidean distance (ED) between two patterns Φ_r and $\Phi_c(k)$. If the pattern Φ_r is similar to any comparative pattern $\Phi_c(k)$, the index $ED(k)$ will be small values. These indexes are used to measure the relationship between the reference and comparative patterns that can be used for pattern relation analysis.

In this study, CRA is designed to detect power quality problems, including harmonics, voltage sag, voltage swell, and voltage interruption. Overall indexes $ED(k)$, k=1, 2, 3, …, K, are converted to gray grade $\rho(k)$ by non-linear transformation, as

$$\rho(k) = \xi \exp[-\xi ED(k)] \tag{16}$$

where ξ is the recognition coefficient with interval $(0,\infty)$. Equation (16) is used to enhance the contrast in indexes $ED(k)$. Intensity adjustment is a technique for mapping an original intensity value to a new specific range. The range of the gray grade $\rho(k)$ is in the interval $[0, \xi]$ as shown in Fig. 1. The coefficient ξ is selected to >>1 in order to make gray grades more distinguishable [16], ξ=5 is chosen in this study. These gray grades can be separated into seven classes: normal (*nor*), harmonic (*h*), swell (*sw*), sag (*sa*), voltage interruption (*int*), swell involving harmonic (*hsw*), and sag involving harmonic (*hsa*), and can be represented as

$$\Gamma=[\rho^{nor}(1), \ldots, \rho^{nor}(N_{nor})|\rho^{h}(1), \ldots, \rho^{h}(N_h)|\rho^{sw}(1), \ldots, \rho^{sw}(N_{sw})|\rho^{sa}(1), \ldots, \rho^{sa}(N_{sa})|\rho^{int}(1), \ldots, \rho^{int}(N_{int})|$$

$$\rho^{hsw}(1), \ldots, \rho^{hsw}(N_{hsw})|\rho^{hsa}(1), \ldots, \rho^{hsa}(N_{hsa})]. \tag{17}$$

Compute the average grade for each class, as

$$\rho_{ave}^{class} = \frac{\sum_{t=1}^{N_{class}} \rho^{class}(t)}{N_{class}} \tag{18}$$

where $class \in [nor, h, sw, sa, int, hsw, hsa]$; N_{class} is the number of each class. Then find the minimum and maximum average grades, as

$$\rho_{\min} = \min[\rho_{ave}^{nor}, \rho_{ave}^{h}, \rho_{ave}^{sw}, \rho_{ave}^{sa}, \rho_{ave}^{int}, \rho_{ave}^{hsw}, \rho_{ave}^{hsa}] \tag{19}$$

$$\rho_{\max} = \max[\rho_{ave}^{nor}, \rho_{ave}^{h}, \rho_{ave}^{sw}, \rho_{ave}^{sa}, \rho_{ave}^{int}, \rho_{ave}^{hsw}, \rho_{ave}^{hsa}] \tag{20}$$

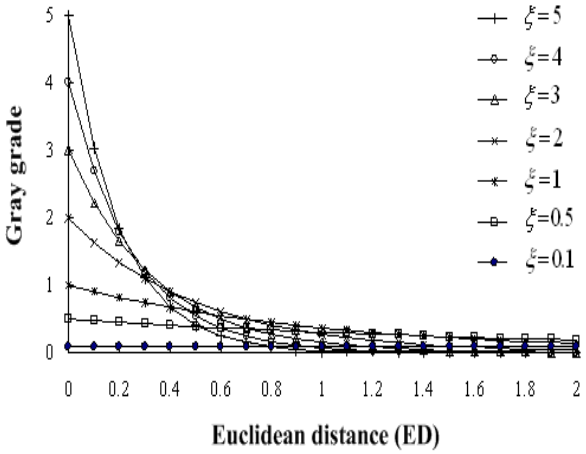

Fig. 1 Euclidean distances versus gray grades

where $\rho_{\min} \neq \rho_{\max}$. According to HSV color model, CRA is defined mathematically by transformations between the RGB color space and the HSV color space. Find the hue angle $H \in [0,360]$ for HSV color space, as

$$H = \begin{cases} 0 \text{ or } 360, & \rho_{\max} = \rho_{ave}^{int} \\ 120 - 60 \times \left(\frac{\rho_{ave}^{hsa} - \rho_{ave}^{nor}}{\rho_{\max} - \rho_{\min}}\right), & \rho_{\max} = \rho_{ave}^{hsa} \\ 120, & \rho_{\max} = \rho_{ave}^{sa} \\ 180, & \rho_{\max} = \rho_{ave}^{nor} \\ 180 \pm 30 \times \left(\frac{\rho_{ave}^{h} - \rho_{ave}^{nor}}{\rho_{\max} - \rho_{\min}}\right), & \rho_{\max} = \rho_{ave}^{h} \\ 240, & \rho_{\max} = \rho_{ave}^{sw} \\ 240 + 60 \times \left(\frac{\rho_{ave}^{hsw} - \rho_{ave}^{nor}}{\rho_{\max} - \rho_{\min}}\right), & \rho_{\max} = \rho_{ave}^{hsw} \end{cases} \tag{21}$$

Find saturation S and value V are defined as

$$V = \rho_{\max} \tag{22}$$

$$S = 1 - \frac{\rho_{\min}}{V} \quad (\rho_{\max} \neq 0) \tag{23}$$

The value of H is generally normalized to lie between 0° and 360°, and hue H has no geometric meaning when $\rho_{min}=\rho_{max}$ and saturation S is zero. For PQ detection, parameter H is employed to identify the seven classes as angle points for nor, *h*, *sw*, *sa*, *int*, *hsw*, and *hsa*, as shown in Fig. 2.

The concept of proposed CRA is derived from HSV color model, which attempts to describe perceptual color relationships for PQ disturbances. Its model is commonly used in computer graphics applications, and stands for hue (H), saturation (S), and value (V), with H depicting as a three-dimensional conical formation of the color wheel as shown in Fig. 2. The S is represented by the distance from the center of a circular cross-section of the cone, and V is adjusted with brightness bar between black and white [18]-[19].

Open Science Index, Energy and Power Engineering Vol:4, No:5, 2010 waset.org/Publication/12617

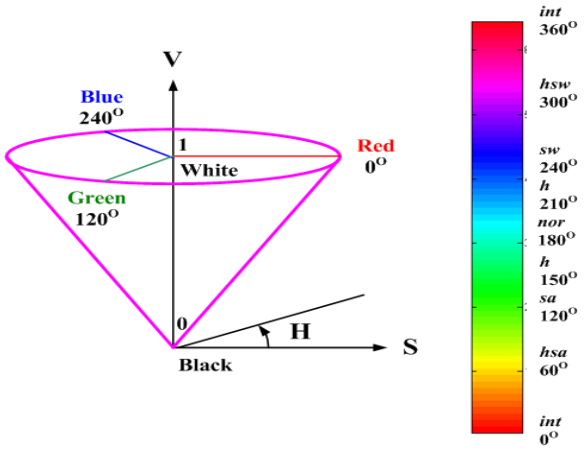

Fig. 2 HSV color space model

In this study, H is employed to identify the grade of disease, and *S* and *V* are the confidence index for recognition results. These two parameters could enhance the reliability of diagnostic results. Its value is great than 0.5 and approach to 1.0, and we will have high confidence to confirm the possible grade.

III. Feature Extraction and Fractal Pattern Creation

The simulation studies of power quality variations are considered including harmonics and voltage fluctuation phenomena. Harmonic events are periodic voltage variations and do not involve variations in the fundamental frequency (60Hz) voltage, which are mostly caused by electronic equipment and nonlinear loads. These events may occur with a long duration (greater than 1 minute), and distortion level is accomplished to characterization with long duration recording and statistics. Voltage fluctuation phenomena, such as voltage swell, voltage sag, and voltage interruption, could occur due to lightning, capacitor switching, large motor starting, nearby circuit faults (short circuit and single-line-to-ground fault), or accidents, and can also lead to power interruptions. These voltage variations are momentary low voltage, high voltage, or voltage interruption in the fundamental frequency voltage that last less than 1 minute. Voltage sag is a sudden voltage drop between 10%~90% in magnitude. It often lasts for 0.5 cycles to 1 minute. When the voltage drops 30% or more, we consider the system status are severe. Voltage swell is a voltage rise above 110% of the normal voltage. Voltage interruption is defined voltage magnitude is less than 10% of nominal lasting for 0.5 cycles to 5 minutes. In a power system, each bus may have disturbances involving harmonics (*h*), voltage sags (*sa*), voltage swells (*sw*), sags or swells involving harmonics (*hsa*/*hsw*), and voltage interruptions (*int*).

A 14-bus system is used for test example as shown in Fig. 3 [9]-[10]. The system has 5 generator buses, 15 lines, 5 transformers, and 8 non-linear devices. There are 8 observation locations in this system. Table I shows the harmonic current components of each harmonic source by field test. At each observation location, harmonic and voltage fluctuation phenomena are considered, as well as the harmonic source causing voltage distortion for neighboring buses. With harmonic power flow, we can simulate harmonic voltages at selected observation locations. We can also consider various harmonic load combinations and work durations at each observation location, i.e. load combinations {Bus13}, {Bus13, Bus6}, {Bus13, Bus11}, {Bus13, Bus12}, {Bus13, Bus6, Bus11}, {Bus13, Bus6, Bus12}, {Bus13, Bus11, Bus12} at Bus13. Comparative patterns can be systematically collected at Bus13 with fractal patterns as (13). Each pattern is conducted within the period of sampling data from distorted waves. The sample rate we consider is 1.44kHz, and the number of sample points is 24 (N=24). Equations (5), (6), and (11) with sequencing preprocess is applied on various distorted waves for extraction features.

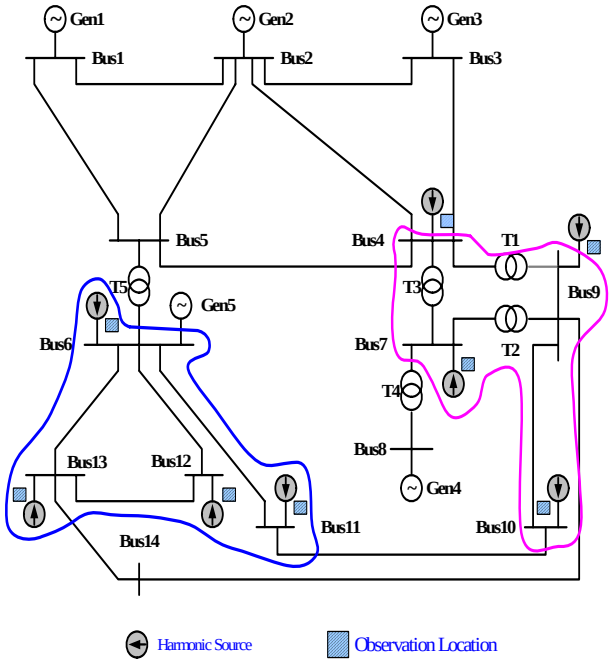

Fig. 3 One-line diagram of the 14-bus power system

TABLE I
HARMONIC CURRENT COMPONENTS AT EACH OBSERVATION LOCATION

Bus No.	Non-linear Device	Harmonic Components
7, 11, 13	6-pulse Rectifier	5, 7, 11, 13, 17, 19, …
4, 6	12-pulse Rectifier	11, 13, 23, 25, …
9	Static Frequency Converter	5, 7, 11, 13, 17, 19, 23, 25, …
10	Thyristor-controlled Reactor	3, 5, 7, 9, 11, 13, …
12	DC Motor	5, 7, 13, 17, 19, 23, …

For a normal voltage signal, one cycle waveform can be divided into two segments, such as positive half-cycle (PHC) and negative half-cycle (NHC), segment number p=1, 2, and sampling points N_p=12 (N=N_1+N_2=24) in each segment. The FD is computed using (7) as D=1log$_{10}$(N)/1log$_{10}$(N_d)=1.2789, where N=24 and N_d=12. D is a parameter between 1 and 2 for processing one-dimensional signals. The remaining map parameters c_p, d_p, f_p, and g_p can be solved by (9) and (10) with 24 sampling points as shown in Table II. Fractal patterns are constructed by using 24 NIFs with the same remaining map parameters in each segment. These fractal patterns have various morphologies that could be used for PQ detection as shown in Fig. 4. For a normal voltage signal, a straight line that passes through the interpolation fractal values and is linear on each segment, respectively. The

Open Science Index, Energy and Power Engineering Vol:4, No:5, 2010 waset.org/Publication/12617

patterns reveal the curves for voltage fluctuations, and the saw-tooth lines for harmonic and harmonic involving voltage fluctuations.

TABLE II
THE REMAINING MAP PARAMETERS OF NIF

FD	The Number of NIF			Remaining Map Parameter			
				c_p	d_p	f_p	g_p
1.2789	*PHC*	φ_{1t}	12	0.6605	2.9926	3.9972	1.5551
	NHC	φ_{2t}	12	-0.6081	3.0360	-4.0610	-1.4390

Note: *PHC*: positive half-cycle; *NHC*: negative half-cycle; N_p: the number of sampling points in each segment, t=1, 2, 3, …, N_p (N_p=12).

According to the various fractal patterns, these patterns can be divided into seven groups, and the numbers of patterns from the same groups are 1-set (N_{nor}=1), 1-set (N_h=1), 6-set (N_{sa}=1), 6-set (N_{sw}=1), 6-set (N_{hsa}=6), 6-set (N_{hsw}=6), and 2-set (N_{int}=2) data, respectively. The number of comparative patterns is equal to 28-set data (K=28). Overall fractal patterns are shown in Fig. 5, and fractal values are inside the interval [1.5 6.0]. Then CRA is used to identify the grade of PQ disturbances, and the possible grade can be presented as an angle point H by (21). Matlab colormap function is used to display the results in the HSV color space. It converts the HSV image to the equivalent RGB image whose three planes contain the red, green, and blue components for the image. The colormap for angle point H could be displayed as an image form 0° to 360° and used in computer graphics application. The values of S and V are in the interval [0,1] as (22) and (23). A threshold value 0.5 is designed for parameter S to separate normal from abnormal values, where a value close to 1 means "*Abnormal*", and 0 means "*Normal*", and indicates the possible disturbing events at observation location. This confirms that results have higher confidence value in the tests.

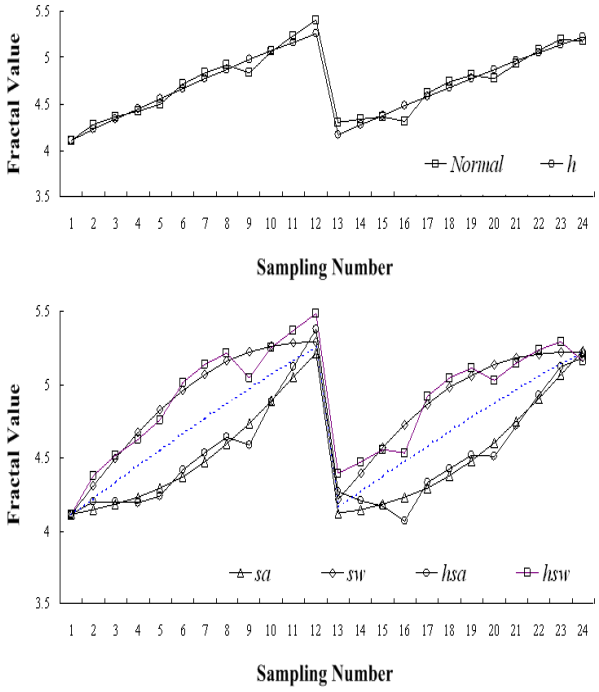

Fig. 4 Various fractal patterns for PQ disturbances

IV. Simulation Results and Discussion

The proposed detection method was designed on a PC Pentium-IV 2.4GHz with 480MB RAM and Matlab software. To show the effectiveness of the proposed method, multiple harmonics and voltage sag involving harmonics were chosen for demonstration. In a 14-bus system, most harmonics are related to power rectifiers or converters, as shown in Fig. 3. With fundamental and harmonic power flow for various loading combinations, bus voltages can be calculated at eight observation locations [20]. At each observing location, we have 28-set of comparative patterns for the NIFs and CRA with following events: normal (*nor*), *h*, *sa*, *sw*, *hsa*, *hsw*, and *int*. Time-domain analysis was conducted to detect the distorted waves with 50 cycles.

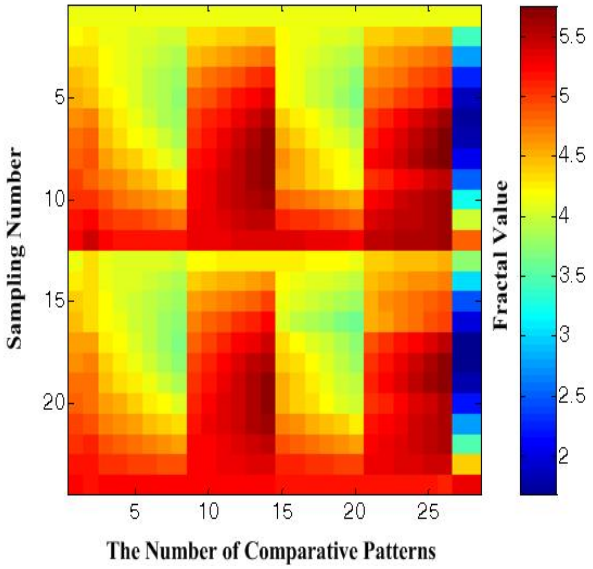

Fig. 5 Various fractal patterns for PQ disturbances

Periodic sampling was done with sampling rate f=1.44*kHz* and sample points N=24. With multiple harmonic sources at Bus6, Bus9, Bus12, and Bus13, sampled data were then applied to each classifier for detection disturbances. For comparison purposes, we have also applied the AWN composed of 24 Morlet wavelets in the wavelet layer and ANN [9]-[10] Tests will show accurate discrimination, for detecting disturbing events.

A. Voltage Sag involving Harmonics

Harmonic measuring should be performed from time to time at selected observation locations. *THD* is used to define the total harmonic voltage distortion. It is commonly used in low, medium, and high voltage power systems. When the periodic sampling data are provided, find the buses with V_{THD}≥2.5%. Then each classifier at an observation location will act to detect the disturbances. Voltage sag (*sa*) may be caused by the switching operations, starting of large motor loads, and nearby circuit faults. Long duration voltage sags down to 80% are caused by heavy loads or faults, with a typical duration up to 10sec. The voltage sags down to 70% are caused by heavy load switching or faults, with a typical duration up to 30 cycles. Let the voltage sags caused by heavy motor loads at Bus13, and multiple harmonic sources are at

Open Science Index, Energy and Power Engineering Vol:4, No:5, 2010 waset.org/Publication/12617

the Bus6, Bus9, and Bus12. Using 50 cycle voltage signals, the harmonics involving voltage sag as drop 14% and detection results are shown in Fig. 6. Results show the times for starting and ending of harmonics in work duration and voltage sag about 30 cycles. The Matlab colormap function presents the hue angles *H* as colors. The results confirm the events are "harmonics (*h*)" and "harmonics involving voltage sag (*hsa*)", and the colormap function presents the average hue angle H_{ave}= 199.47° (cyanine series) for "event *h*" and H_{ave}= 60.98° (yellow series) for "event *has*", respectively. The average confidence value is greater than 0.5 means agree to certain PQ disturbances. This confirms that the proposed classifier has a higher confidence value of detection results in the tests.

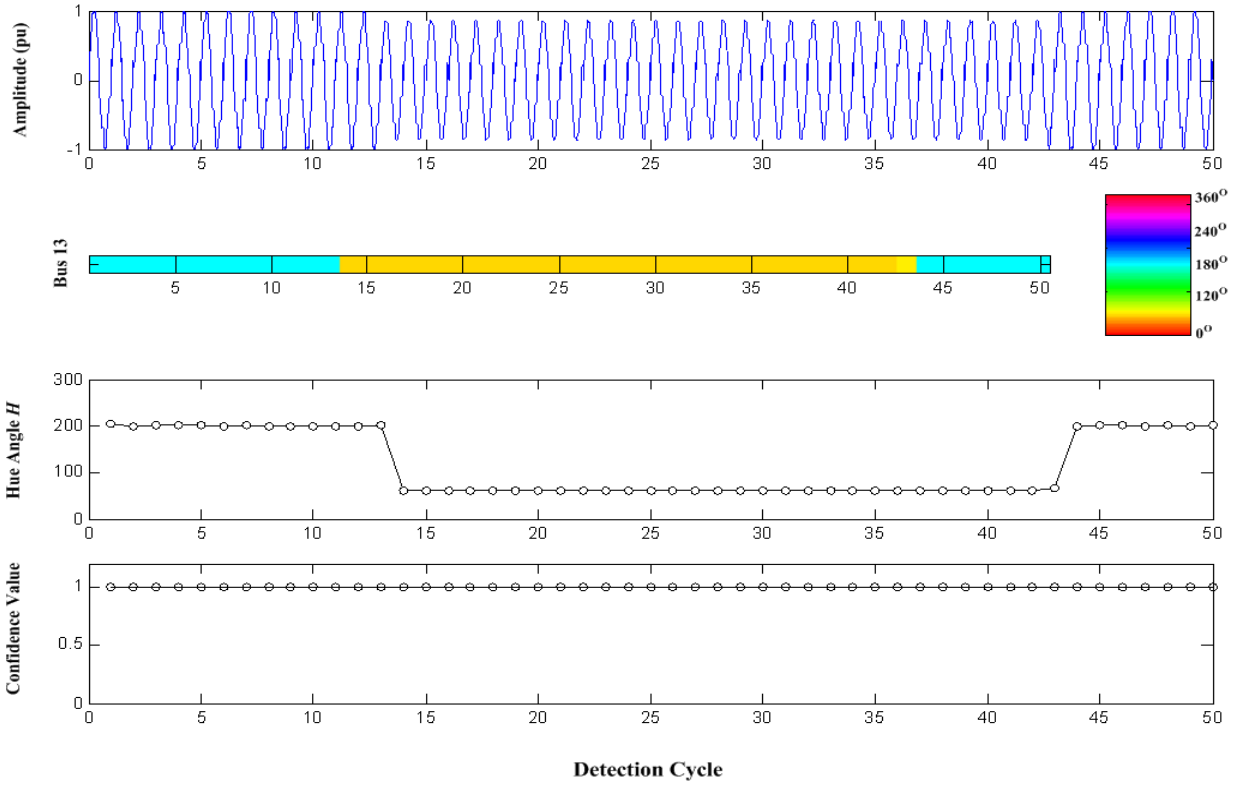

Fig. 6 Time-domain voltage signals and detection results

B. Comparison of CRA with WNN

For classification applications, wavelet neural network (WNN) has also presented for this study. Table III shows the related data and comparison of CRA classifier with WNN classifier. The architecture of WNN is 24-55-5-4, including 24 wavelet nodes, 55 hidden nodes, 5 summation nodes, and 4 output nodes [9]-[10]. The methods CRA and WNN have the promising results for PQ detection. However, steepest descent algorithm was used to adjust the network parameters to enhance detection accuracy. As the number of training data increases, training process and classification efficiency become a main problem. Wavelet transformation (WT) cascades filters (low-pass or high-pass filters) and down/up-sampling operations to generalize several frequency bands. Significant features are suited to classify different signals at specific dilation and translation parameters. It is decomposed into several components using dilated (scale) and

translated (time) version of prototype wavelet. The WT could affect reconstructed signal quality, the wavelet coefficients need to be chosen. Significant features are suited to classify different patterns with a trial procedure of wavelet decomposition and experiences. The CRA classifier has the straightforward mathematical operation to process numerical computation, the flexible pattern mechanism with add-in or delete-off the comparative patterns without any retraining process. It is a dynamical modeling system, and the database is continually formed for comparative patterns added or deleted to the current comparative matrix, as can be seen in (13). The outcomes of the proposed classifier are better than WNN-based classifier.

V. Conclusion

CRA classifiers have been proposed to detect PQ disturbances in a power system. NIFs act to extract and enhance the features from voltage signal in the time-domain, including harmonics and voltage fluctuation phenomena. The process results in data self-similarity, thus reducing the amount of datasets required. A GRA classifier uses these distinctive features to classify PQ disturbances. It has a flexible pattern mechanism with add-in and delete-off features without adjusting many parameters. The results can be

Open Science Index, Energy and Power Engineering Vol:4, No:5, 2010 waset.org/Publication/12617

presented in colors in computer graphics application. The saturation parameter is a confidence degree used to confirm the possible event. The proposed classifier provides a promising way for further using in a real-time and an off-line analysis tool, and SCADA/EMS will be integrated without extra devices.

TABLE III
THE RELATED DATA OF CRA AND WNN CLASSIFIER

Method / Task	CRA Classifier	WNN Classifier
Network Architecture	No	According to Input-Output and Training Data ***Note* (1)**
Database	28 Comparative Patterns	55 Input-Output Pairs Training Data
Activation Function	Equation (16)	*Morlet Wavelet* and *Gaussian Activation Function* [9], [10]
Learning Algorithm	No	Steepest Descent Algorithm
Parameter Assignment	Minor Recognition Coefficient $(0,\infty)$	Major *Dilation*, *Translation*, and *Smoothing Parameters* *Learning Rate* (0,1)
Parameter Adjustment	No	Training Iteration ***Note* (2)**
Adaptation Capability	Good *Expandable or Reducible Patterns*	Moderate *Retrain with New Training Patterns*

Note: (1) Wavelet–Hidden-Summation-Output Node: 24-55-5-4; (2) Convergent Conditions: (a) the objective function is less than the pre-specified value; (b) the number of iterations achieve the maximum allowable number.

REFERENCES

[1] IEEE Recommended Practices for Monitoring Electric Power Quality ANSI/IEEE Std. 1159-1995.
[2] Kwan, T. and Martin, K., "Adaptive Detection and Enhancement of Multiple Sinusoids Using a Cascade of IIR Filters, "IEEE Trans., 1989, CAS-36, pp. 936-947.
[3] E. O. Brigham, "The Fast Fourier Transform, "Englewood Cliffs, NJ: Prentice-Hall, 1990.
[4] P. Pillay and A. Bhattacharjee, "Application of Wavelet to Model Short-Term Power System Disturbances, "IEEE Trans. on Power System, Vol. 1, No. 4, November 1996, pp. 2031-2037.
[5] L. Angrisani, P. Daponte, M. D' Apuzzo, and A. Testa, "A Measurement Method Based on the Wavelet Transform for Power Quality Analysis, "IEEE Trans. on Power Delivery, Vol. 13, No. 4, October 1998, pp. 990-998.
[6] S. Santoso, E. J. Powers, and W. M. Grady, "Power Quality Disturbance Identification Using Wavelet Transforms and Artificial Neural Networks, "Proc. of the 1996 IEEE Int. Conf. on Harmonics and Quality of Power, Las Vegas, NV, USA, October 16-18 1996, pp. 615-618.
[7] Leopoldo Angrisani, Pasquale Daponte, and Massimo D' Apuzzo, "Wavelet Network-Based Detection and Classification of Transients, "IEEE Trans. on Instrumentation and Measurement, Vol. 50, No. 5, October 2001, pp. 1425-1435.
[8] Shyh-Jier Huang, tasi-Ming Yang, and Jiann-Tseng Huang, "FPGA Realization of Wavelet Transform for Detection of Electric Power System Disturbances, "IEEE Transactions on Power Delivery, Vol. 17, No. 2, April 2002, pp. 388-394.
[9] Chia-Hung Lin and Ming-Chieh Tsao, "Power Quality Detection with Classification Enhancible Wavelet-Probabilistic Network in a Power System, "IEE Proceedings-Generation, Transmission, and Distribution, Vol. 152, No. 6, November 2005, pp. 969-976.
[10] Chia-Hung Lin and Chia-Hao Wang, "Adaptive Wavelet Networks for Power Quality Detection and Discrimination in a Power System, "IEEE Transactions on Power Delivery, Vol. 21, No. 3, July 2006, pp. 1106-1113.
[11] Michael Barnsley, "Fractal Functions and Interpolation, "Constructive Approximation, 2:303-329, 1986.
[12] M. E. Kirlangic, D. Perez, S. Kudryavtseva, G. Griessbach, G. Henning, G. Ivanova, "Fractal Dimension as a Feature for Adaptive Electroencephalogram Segment in Epilepsy, "2001 Proceedings of the 23rd Annual EMBS International Conference, October 25-28, Istanbul, Turkey, pp. 1573-1576.
[13] D. S. Mazel and M. H. Hayes, "Using Iterated Function Systems to Model Discrete Sequences, "IEEE Transaction on Signal Processing, Vol. 40, No. 7, July 1992, pp. 1724-1734.
[14] Greg Vines and Monson H. Hayes, III, "Nonlinear Address Maps in a One-Dimensional fractal Model, "IEEE Transactions on Signal Processing, Vol. 41, No. 4, April 1993, pp. 1721-1724.
[15] Rosana Esteller, George Vachtsevanos, Javier Echauz, and Brian Litt, "A Comparison of Waveform Fractal Dimension Algorithm, "IEEE Transactions on Circuits and Systems Fundamental Theory and Applications, Vol. 48, No. 2, February 2001, pp. 177-183.
[16] Chia-Hung Lin, Yi-Chun Du, and Tainsong Chen, "Nonlinear Interpolation Fractal Classifier for Multiple Cardiac Arrhythmias Recognition, "Chaos, Solitons, & Fractals Applications in Science and Engineering, Vol. 42, No. 4, 30 November 2009, pp. 2570-2581.
[17] Chia-Hung Lin, "Classification Enhancible Grey Relational Analysis for Cardiac Arrhythmias Discrimination, "Medical & Biological Engineering & Computing, Vol. 44, No. 4, April 2006, pp. 311-320.
[18] Donald Hearn and M. Pauline Baker, "Computer Graphics, "Prentice Hall International, 1986, ISBN 0-13-165598-1.
[19] Rafael C. Gonzales and Richard E. Woods, "Digital Image Processing, "Prentice Hall Press, 2002, ISBN 0-201-18075-8.
[20] Y.H. Yan, C.S. Chen, C.S. Moo, and C.T. Hsu, "Harmonic Analysis for Industrial Customer, " IEEE Transactions on Power Delivery, Vol. 30, No.2, March/April 1994, pp. 462-468.

Chia-Hung Lin was born in 1974. He received the B.S. degree in electrical engineering from the Tatung Institute of Technology, Taipei, Taiwan, in 1998, the M.S. degree in electrical engineering from the National Sun Yat-Sen University, Kaohsiung, Taiwan, in 2000, and the Ph.D. degree in electrical engineering from National Sun Yat-Sen University in 2004. Currently, he is an Associate Professor of department of electrical engineering, Kao-Yuan University, Lu-Chu Hsiang, Kaohsiung, Taiwan, where has been since 2004.

His research interests include fault diagnosis in power system, neural network computing, and harmonic analysis. Currently, his area of interest is biomedical signal processing and pattern recognition.

Mei-Sung Kang received the M.S., Ph.D. degree in Electrical Engineering from the National Sun Yat-Sen University in 1993 and 2001 respectively. Since August 1993, he has been with Department of Electrical Engineering, Kao Yuan Institute of Technology, Kaohsiung, Taiwan. Currently he is a professor of department of electrical engineering, Kao-Yuan University.His research interest is in the area of load survey and demand subscription service.

Cong-Hui Huang was born on May 28, 1979. He received the B.S. degree in electrical engineering from the National Taiwan University of Science and Technology, Taipei, Taiwan, R.O.C., in 2001 and the M.S. degree in electrical engineering and Ph.D. degree from the National Sun Yan-Sen University, Kaohsiung, Taiwan, in 2003 and 2008, respectively.

He has been with the Department of Automation and Control Engineering, Far East University, Hsin-Shih, Tainan County, Taiwan, since 2008. His research interests include power system operation, power system security, power deregulation, and intelligent solar control system.

Chao-Lin Kuo received the B.S. degree from the Department of Automatic Control Engineering, Feng Chia University, Taichung, Taiwan, Republic of China, in 1998, and M.S. degree from the Institute of Biomedical Engineering, National Cheng Kung University, Tainan, Taiwan, Republic of China, in 2000. In 2006, he received his Ph.D. degree in Department of Electrical Engineering, National Cheng Kung University, Tainan, Taiwan, Republic of China. He has been with the Department of Electrical Engineering, Far East University since 2004, and is currently an assistant Professor. His current research interests include intelligent control systems, fuzzy systems, and embedded systems and its applications.

Open Science Index, Energy and Power Engineering Vol:4, No:5, 2010 waset.org/Publication/12617